

Radiative Capture of Protons by Be⁹†

W. E. MEYERHOF,* *Department of Physics, Stanford University, Stanford, California,*
 N. W. TANNER,‡ *Kellogg Radiation Laboratory, California Institute of Technology, Mount Wilson and Palomar Observatories,*
Carnegie Institute of Washington, California Institute of Technology, Pasadena, California,

AND

C. M. HUDSON,§ *Office of the Chief of Ordnance, Department of the Army, Washington, D. C.*

(Received April 13, 1959)

The gamma rays from the capture in Be⁹ of protons of energy between 0.27 and 1.2 Mev have been studied using large scintillation crystals. Excitation functions of the gamma rays leading to the 0-, 0.72-, 1.74-, 2.15-, 3.58-, and 5.16-Mev states of B¹⁰ were computed from the measured gamma-ray spectra. In addition to the resonances previously known to exist at 0.33-, 0.99-, and 1.086-Mev proton energy [corresponding to (1⁻) 6.88-, (2⁻) 7.48-, and (0⁺) 7.56-Mev states in B¹⁰], evidence was found only for the *p*-wave resonance near 1 Mev [(2⁺) 7.5-Mev state in B¹⁰] postulated by Mozer and by Dearnaly and for the influence of higher lying states. This work leaves unexplained the large isotopic-spin impurity of the 6.88-Mev level. Appreciable nonresonant capture was found for the transitions to the 0-, 0.72-, 3.58-, and 5.16-Mev states, which is probably not *s*-wave for the latter two transitions. Accurate energy measurements and coincidence work showed that the 5.16-Mev level of B¹⁰ is populated in preference to the 5.11-Mev level, contradicting earlier work of Clegg. Also, experimental evidence has been found which appears to be in contradiction to the 0⁺ spin assignment for the 7.56-Mev level of B¹⁰ and raises doubts about the 2⁺ spin assignment of the 5.16-Mev level.

I. INTRODUCTION

IN a recent paper¹ certain speculations were made about the levels of B¹⁰ which could be the isotopic-spin analogs of the levels in Be¹⁰ located at² 5.96, 6.18, and 6.26 Mev. Evidence was presented¹ which indicated that the spins of the 5.96- and 6.26-Mev levels of Be¹⁰ were 1⁻ and 2⁻, respectively. On the other hand in B¹⁰ a spin 1⁻ level was known² to exist at 6.88 Mev and presumably spin 2⁻ levels were known² to lie at 7.48 and 7.78 Mev, which could be the analog levels of the aforementioned Be¹⁰ levels.

The high isotopic-spin impurity³ of the 1⁻ 6.88-Mev level of B¹⁰ makes it appear likely^{1,4} that another 1⁻ level should lie close to it. The present work was motivated by an attempt to search for such a level using the Be⁹(*p*, γ)B¹⁰ reaction. During the course of our experiments we were informed of the work of Edge and Gemmell⁴ on the same reaction, motivated in a similar fashion. In our work protons of energy between 0.27 and 1.20 Mev were used (corresponding to an excitation energy of B¹⁰ between 6.83 and 8.67 Mev);

in the work of Edge and Gemmell protons of energy between 0.22 and 0.44 Mev were used.

We can mention already here that our work has not indicated any second 1⁻ level in B¹⁰ in the energy region which was surveyed. Furthermore, our work may have left more questions unanswered than were in our mind previously, with respect to the 3-kev wide 7.56-Mev state of B¹⁰, whose gamma decay we also investigated. Nevertheless, since a Van de Graaff machine is not available to us at this time we believe that it is of general interest to publish our results now, in order to stimulate further work on the excited states of B¹⁰.

II. EXPERIMENTAL METHODS

All the gamma-ray spectra were measured with a NaI(Tl) crystal, 4 in. in height and 4 in. in diameter, and displayed on a RIDL 100-channel pulse-height analyzer. The gamma rays were collimated by a 1½-in.

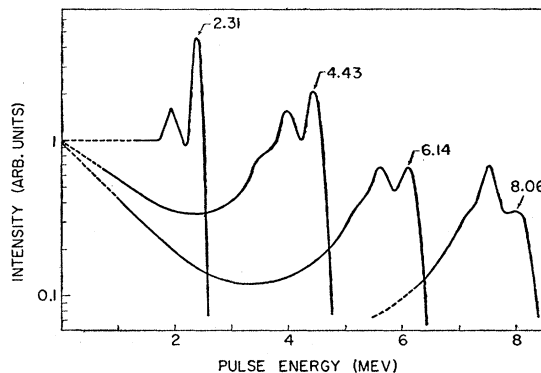


FIG. 1. Typical pulse-height distributions from the 4-in. x 4-in. NaI(Tl) crystal used with a 1½-in. diam lead collimator, 4 in. long. The energies of the single gamma rays are given in Mev. (2.31 should read 2.38.)

† Assisted in part by a grant of the Alfred P. Sloan Foundation, Inc., to Stanford University and by the joint program of the Office of Naval Research and the U. S. Atomic Energy Commission at the California Institute of Technology and at Stanford University. Experimental work performed at the Kellogg Radiation Laboratory, California Institute of Technology.

* Alfred P. Sloan Foundation Fellow, 1957-1958. Senior Research Fellow at the California Institute of Technology, 1957-1958.

‡ Present address: The Clarendon Laboratory, Oxford, England.

§ Research Associate at Stanford University, Summer 1958.

¹ W. E. Meyerhof and L. F. Chase, Jr., *Phys. Rev.* **111**, 1348 (1958).

² F. Ajzenberg and T. Lauritsen, *Nuclear Phys.* **11**, 1 (1959).

³ D. H. Wilkinson and A. B. Clegg, *Phil. Mag.* **1**, 291 (1956); A. B. Clegg, *Phil. Mag.* **1**, 1116 (1956).

⁴ R. D. Edge and D. S. Gemmell, *Proc. Phys. Soc. (London)* **71**, 925 (1958).

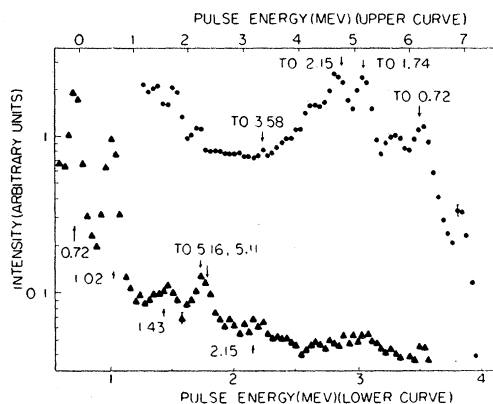


FIG. 2. Gamma-ray spectrum of $\text{Be}^9 + p$ at 0.33 Mev. Low- and high-gain curves are shown. The arrows mark the energies at which capture gamma rays to excited states of B^{10} are expected. On the lower curve energies of expected secondary gamma rays are also marked. Typical statistical errors are indicated.

diameter hole in a 4-in. thick lead shield and entered the crystal along the cylinder axis. For general orientation we give in Fig. 1 four pulse-height spectra measured in the above geometry for single gamma rays of 2.38-, 4.43-, 6.14-, and 8.06-Mev energy, produced in the reactions $\text{C}^{12}(p, \gamma)$ ($E_p = 0.47$ Mev); $\text{N}^{15}(p, \alpha \gamma)$ ($E_p = 0.90$ Mev), $\text{F}^{19}(p, \alpha \gamma)$ ($E_p = 0.62$ Mev), and $\text{C}^{13}(p, \gamma)$ ($E_p = 0.55$ Mev), respectively.

Several Be targets were made which had thicknesses of less than 20 kev at proton bombardment energy. The targets were evaporated on carefully cleaned copper disks, which were mounted $1\frac{1}{4}$ in. in front of the gamma-ray collimating channel. After some trials, the targets could be made essentially free of fluorine contamination.

For coincidence work, the collimator was removed and two 4-in. \times 4-in. NaI(Tl) crystals were used at a distance of approximately 2 in. from the target. A conventional coincidence circuit was used to gate the 100-channel analyzer.

The single gamma-ray spectra were measured at 90°

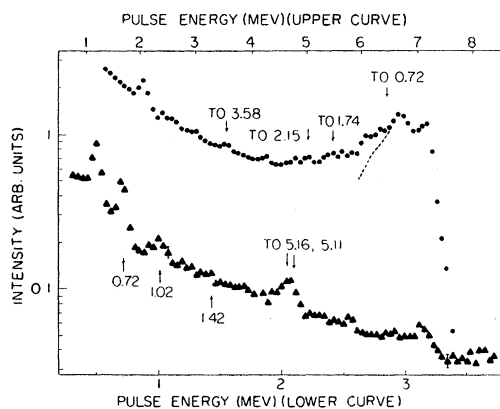


FIG. 3. Gamma-ray spectrum of $\text{Be}^9 + p$ at 0.65 Mev. For significance of markings, see caption to Fig. 2.

with respect to the proton beam, except at 0.65-Mev proton energy where a 0° spectrum was also measured. Spectra were usually measured with two different amplifier gains, to cover the entire gamma-ray spectrum from 0.5 to 8 Mev. The gamma-ray spectra were analyzed (after subtraction of room background) in the conventional manner of subtracting successive single gamma-ray spectra starting with the highest-energy gamma rays. It can be seen in the typical spectra shown below that, except for a region between $2\frac{1}{2}$ - and $3\frac{1}{2}$ -Mev pulse energy, the analysis of the gamma-ray data is quite unambiguous. The photopeak areas with appropriate corrections for detection efficiency and absorption (including differential penetration of the edges of the lead collimator) were used in order to obtain the gamma-ray intensities. At each proton energy the gamma rays were fitted into the known levels² of B^{10} and a check was made to see that the high- and low-energy gamma-ray intensities

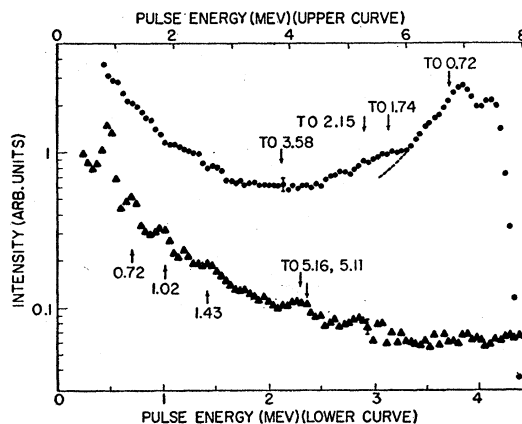


FIG. 4. Gamma-ray spectrum of $\text{Be}^9 + p$ at 0.99 Mev. For significance of markings, see caption to Fig. 2.

balanced. This balance was usually exact to within 20%, except for the alpha-particle unstable level at 5.16 Mev.

III. RESULTS

(a) Single Gamma-Ray Spectra

Figures 2 to 4 show three typical single gamma-ray spectra (at 0.33-, 0.65-, and 0.99-Mev proton energy, respectively), out of the spectra taken at twenty different proton bombardment energies between 0.27 and 1.20 Mev. (The spectra at 0.99 Mev were taken with a freshly mounted crystal, for which the pulse-height spectra in Fig. 1 are not strictly applicable.) It can be seen that at the lower bombardment energies well-defined peaks due to the high- and low-energy gamma rays appear. At the higher bombardment energies the strong gamma ray to the ground state of B^{10} made the analysis of other higher energy gamma rays difficult (see also reference 5) so that the analysis had to rely mainly on the lower energy gamma rays.

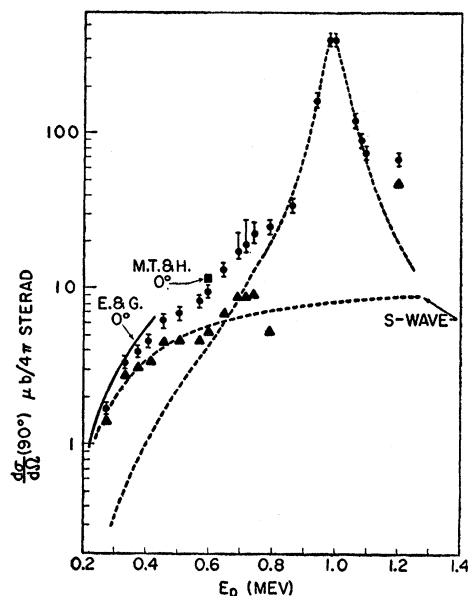


FIG. 5. Excitation curve of gamma ray to ground state ($J^\pi=3^+$, $T=0$) of B^{10} in Be^9+p at 90° to proton beam. Measurements at 0° are from reference 4 (E. and G.) and one point from the present work (M.T. and H.). The calculated Breit-Wigner resonance curve for the 0.99-Mev resonance is indicated. After subtraction of this curve from the experimental values, the points marked by triangles are obtained. An s-wave penetrability curve is indicated. See text for discussion.

The analysis of the single gamma-ray spectra enabled us to show that proton-capture gamma rays exist to the 0-, 0.72-, 1.74-, 2.15-, 3.58-, and 5.16-Mev levels of B^{10} . The excitation curves for these gamma rays are shown in Figs. 5 to 10. Figure 11 shows the excitation curves of some of the secondary gamma rays. The differential cross section of the ground-state gamma ray

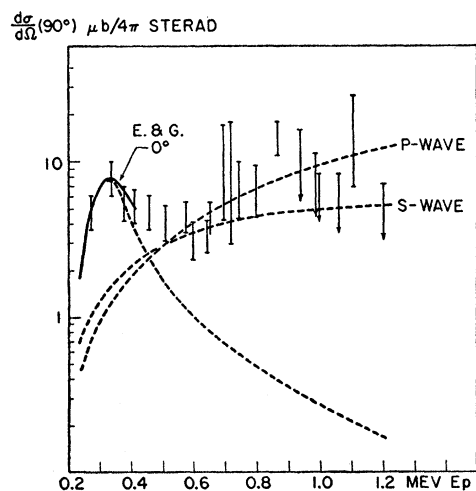


FIG. 6. Excitation curve of gamma ray to 0.72-Mev state ($J^\pi=1^+$, $T=0$) of B^{10} in Be^9+p at 90° to proton beam. Measurements at 0° are from reference 4 (E. and G.). Upper limits are indicated by arrows. The calculated Breit-Wigner resonance curve for the 0.33-Mev resonance is indicated, as well as s- and p-wave penetrability curves.

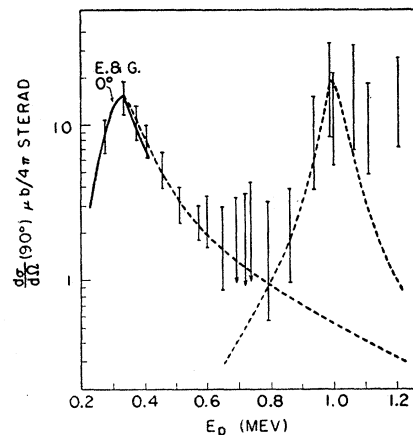


FIG. 7. Excitation curve of gamma ray to 1.74-Mev state ($J^\pi=0^+$, $T=1$) of B^{10} in Be^9+p at 90° to proton beam. Measurements at 0° are from reference 4 (E. and G.). The calculated Breit-Wigner resonance curves for the 0.33- and 0.98-Mev resonance are indicated. Parameters for the latter resonance were taken from Mozer, reference 9. See also reference 10.

was normalized to $400 \mu\text{b}/4\pi$ sterad at 998 kev^{5,6} ignoring the small angular anisotropy²; this was sufficient to normalize all the other differential cross sections. The errors indicated for the differential cross sections include errors in the gamma-ray efficiency calibration as well as consistency errors in the balance of high- and low-energy gamma-ray intensities. At certain proton energies only upper limits for the gamma-ray intensities could be set, particularly for the capture gamma ray⁷ to the 3.58-Mev state of B^{10} .

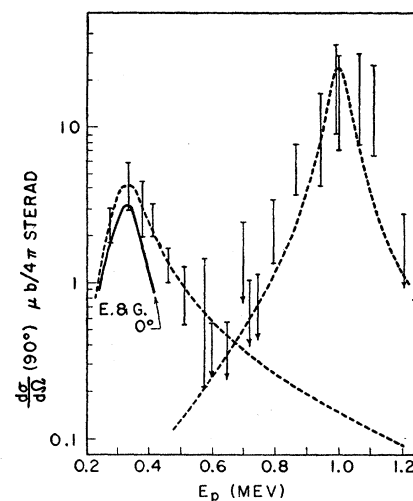


FIG. 8. Excitation curve of gamma ray to 2.15-Mev state ($J^\pi=1^+$, $T=0$) of B^{10} in Be^9+p at 90° to proton beam. Measurements at 0° are from reference 4 (E. and G.). The calculated Breit-Wigner resonance curves for the 0.33- and 0.99-Mev resonance are indicated.

⁵ W. F. Hornyak and T. Coor, Phys. Rev. **92**, 678 (1953).

⁶ N. Jarmie and J. D. Seagrave, Los Alamos Scientific Laboratory Report LA-2014, 1957 (unpublished).

⁷ G. R. Bishop and J. C. Bizot, J. phys. radium **18**, 434 (1957).

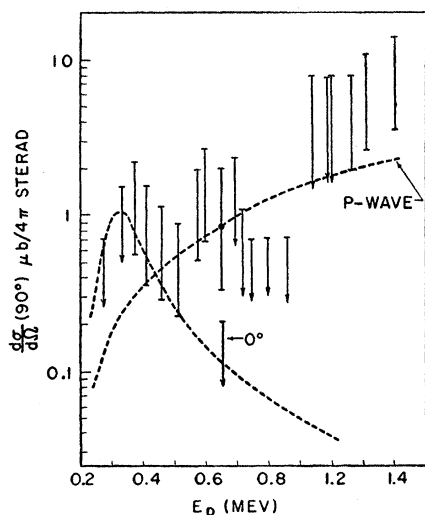


FIG. 9. Excitation curve of gamma ray to 3.58-Mev state ($J^\pi=2^+$, $T=0$) of B^{10} in Be^9+p at 90° proton beam. The 0° measurement at 0.65 Mev is from the present work; the upper limit indicated is to be taken with respect to the 90° point especially marked. The calculated Breit-Wigner resonance curve for the 0.33-Mev resonance is indicated, as well as a p -wave penetrability curve.

At the lower proton energies the results of Edge and Gemmell⁴ are shown, normalized to our values of the intensity of the capture gamma ray to the 1.74-Mev state of B^{10} (since this is the most intense gamma ray at the lower proton energies). It should be noted, though, that the work of Edge and Gemmell was done at 0° to the proton beam, ours at 90° . Only at 0.65-Mev proton energy was a 0° spectrum taken by us and the corresponding results are indicated on Figs. 5, 9, and 10.

As will be seen below, it was of particular interest to show that according to our results the capture gamma

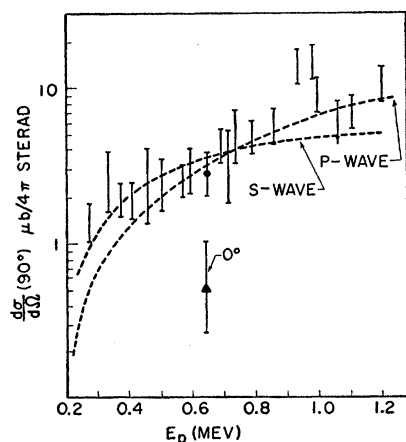


FIG. 10. Excitation curves of gamma ray to 5.16-Mev ($J^\pi=2^-$) state of B^{10} in Be^9+p at 90° to proton beam. The 0° measurement is from the present work; the error indicated is to be taken with respect to the 90° point especially marked. s - and p -wave penetrability curves are indicated. Possible resonance effects at 0.33 and 0.99 Mev are apparent.

rays to the 5.1-Mev states of B^{10} indeed go at least predominantly to the 5.16-Mev state, rather than to the 5.11-Mev state, as reported by Clegg.³ Figure 12 plots the gamma-ray energy measured by us *versus* the proton energy and indicates the expected relationship for a transition to the 5.11-Mev state and to the 5.16-Mev state. It appears from the figure that the gamma radiation goes predominantly to the 5.16-Mev state, a conclusion which is supported by the coincidence work described below.

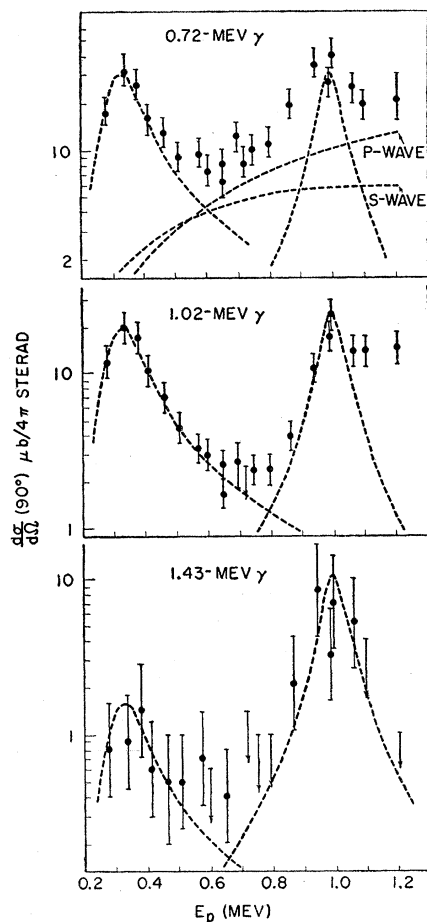


FIG. 11. Excitation curves of secondary gamma rays in Be^9+p at 90° to proton beam. The calculated Breit-Wigner resonance curves for the 0.33- and 0.99-Mev resonances are indicated, as well as s - and p -wave penetrability curves.

As part of our studies, although not directly related to their original motivation, we investigated the gamma decay of the 3-kev wide resonance at 1.086-Mev proton energy.² A 7-kev thick target was used, but only one run was made. Figure 13 shows the gamma-ray spectrum at 1.086 Mev, as well as an average of spectra taken at 1.066 and 1.100 Mev, which should indicate the "background" under the resonant spectrum.

The qualitative analysis of the higher energy gamma rays is somewhat uncertain, but it appears from Fig.

13 that a "resonant" gamma ray of 5.82-Mev energy may be present in the spectrum. Comparison with the gamma-ray spectrum taken with the same crystal at the 0.99-Mev resonance (Fig. 4) shows that the peak at 5.82 Mev is not due to the pair peak of the 6.84-Mev gamma ray. The latter "peak" is indicated by the dotted line in Fig. 13.

A particularly careful energy determination was made for the 2.4-Mev gamma ray shown in Fig. 13. The 2.62-Mev gamma ray of Th C was run simultaneously with the $\text{Be}^9(p, \gamma)$ spectrum at 1.086-Mev proton energy. Figure 14 shows the composite spectrum as well as the spectrum with the Th C gamma ray subtracted out. It can be seen that the energy of the gamma ray in question is more nearly equal to 2.40 Mev, as would be

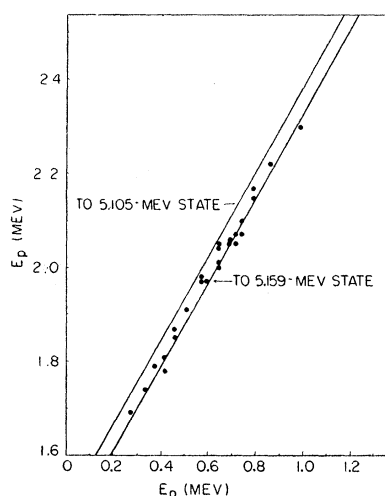


FIG. 12. Energy of capture gamma ray to 5.11- or 5.16-Mev states of B^{10} versus proton energy in $\text{Be}^9(p, \gamma)$ reaction. The two curves indicate the energy relationship expected if capture occurs to the 5.105- or 5.159-Mev states, respectively. The error to be attached to the gamma-ray energy determinations is approximately equal to half the vertical distance between the two lines. It is apparent from these curves that the 5.16-Mev state is at least predominantly populated, which is in agreement with the gamma-gamma coincidence work described in the text.

expected if it is a capture gamma ray to the 5.16-Mev state of B^{10} , than 2.45 Mev, as would be expected for a transition to the 5.11-Mev state. Figure 13 shows that the off-resonant part of the gamma-ray spectrum plays no role in this analysis.

(b) Gamma-Gamma Coincidences

It was desirable to show more definitely than indicated by Fig. 12 that the capture gamma ray, believed by Clegg³ to go to the 5.11-Mev state of B^{10} , goes predominantly to the 5.16-Mev state. This was done by searching for gamma rays which would be in coincidence with the capture radiation in question. Since the 5.11-Mev state has a large alpha-particle width⁸ no gamma rays are expected coincident with a gamma

⁸ L. Meyer-Schützmeister and S. S. Hanna, Phys. Rev. **108**, 1505 (1957).

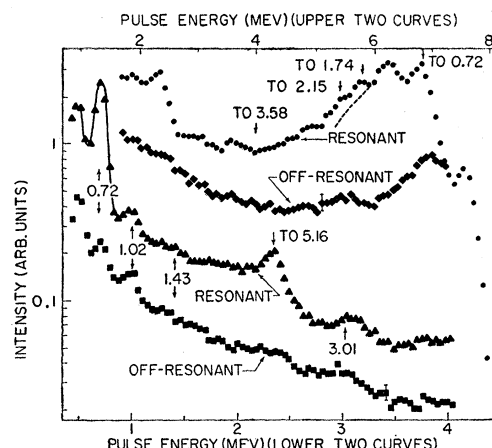


FIG. 13. Gamma-ray spectrum of $\text{Be}^9 + p$ at 1.086 Mev. A 7-kev thick target was used to study this (3 kev wide) resonance. The off-resonant curves are averages of spectra taken at 1.066 and 1.100 Mev and should indicate the counts not to be attributed to the 1.086-Mev resonance. Typical statistical errors are indicated; those for the top curve are no larger than the size of the symbols. Arrows indicate energies at which capture gamma rays to excited states of B^{10} and secondary gamma rays are expected. A transition to the 1.74-Mev state of B^{10} appears to be indicated. See text for discussion.

transition to this state. On the other hand, in the case of the 5.16-Mev state the alpha-particle width is comparable with the gamma width,¹ so that gamma rays are expected to be in coincidence with a gamma tran-

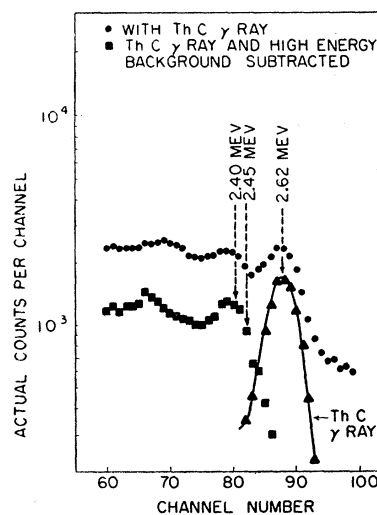


FIG. 14. Energy determination of the capture gamma ray to the 5.11- or 5.16-Mev states of B^{10} at 1.086-Mev proton energy in $\text{Be}^9(p, \gamma)$ reaction. A 2.62-Mev gamma ray (Th C) was run together with the reaction and the resultant points are shown by the top curve. The 2.62-Mev gamma ray (triangles) was subsequently run separately for the same length of time. After subtraction of this gamma-ray distribution as well as of the distribution of Compton electrons from higher energy gamma rays (see Fig. 13), the curve marked by squares was obtained. It is apparent that the photopeak corresponds more nearly to 2.40 Mev, expected for a capture transition to the 5.16-Mev state, than to 2.45 Mev, expected for a transition to the 5.11-Mev state. The asymmetry of the photopeak on the low-energy side can be ascribed to the presence of a 2.15-Mev gamma ray.

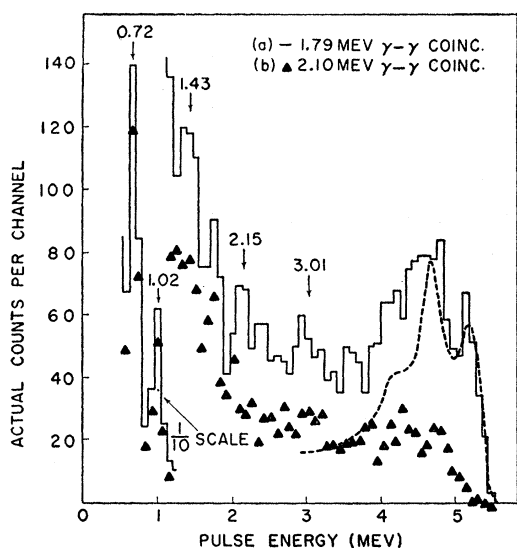


FIG. 15. Gamma-gamma coincidence spectra in $\text{Be}^9(p,\gamma)$ reactions at 0.41-Mev proton energy. The energies at which photopeaks are expected, if the capture gamma ray of 1.79 Mev leads to the 5.16-Mev state of B^{10} , are marked with arrows. The shape expected for a 5.2-Mev gamma ray is indicated in dashed lines. See text for discussion.

sition to this state. The coincident gamma rays would have energies (in Mev) and intensities as follows⁸: 5.16 (7%), 4.44 (29%), 3.01 (64%); furthermore, secondary gamma rays of 2.15-, 1.43-, 1.02-, 0.72-, and 0.41-Mev energy are expected.^{2,8}

Two 4-in. long \times 4-in. diam NaI(Tl) crystals were used for the coincidence work. The crystals were placed about 2 in. from the target, at 90° to the proton beam, and at 180° with respect to each other. At a given proton bombardment energy, a coincident gamma-ray spectrum was first measured with the discriminating channel set on the photopeak of the capture gamma ray of interest and then with the discriminating channel just above the photopeak. In this way we hoped to find out which part of the coincident gamma-ray spectrum was caused by the capture gamma ray and which part was caused by Compton electrons from higher energy gamma rays. In practice it turned out that due to the complexity of the entire gamma-ray decay scheme (and the proximity of the crystals to the target, which caused some solid-angle addition) even the small displacement of the discriminating channel away from the photopeak in question produced gamma-ray coincidences different from those associated with the actual Compton "background" under the photopeak.

Gamma-gamma coincidences were first studied at a proton energy of 0.41 Mev. At this proton energy the capture gamma ray to the 5.16-Mev state of B^{10} has an energy of 1.79 Mev. Hence, the discriminating detector was first set to cover an energy range (a) from 1.70 to 1.90 Mev and then (b) from 2.00 and 2.20 Mev. The same total beam charge was collected in each case. In Fig. 15 curves (a) and (b) show the respective coincident

gamma-ray spectra, with only the chance coincidence background subtracted. The energies at which photopeaks should occur, if the 5.16-Mev level of B^{10} is fed by the capture gamma ray, are marked with arrows. The intense 5.2-Mev gamma ray in curve (a) appeared because the discriminating channel accepted the solid-angle-added pulses of 1.02- and 0.72-Mev energy which were produced by the gamma rays leaving the 1.74-Mev level of B^{10} . (Figure 7 shows that the 1.74-Mev level of B^{10} is strongly populated by direct capture gamma rays at this proton energy.) In curve (b) the discriminating channel was too far above 1.74 Mev for this effect to occur. Despite this spurious effect, it appears from Fig. 15 that coincident gamma rays of 3.0-, 2.1-, and 1.4-Mev energy occur stronger in curve (a) than (b). (A small part of this effect for the latter two gamma rays is caused by the variation of the intensity of the Compton background as the discriminator is shifted.) The reason for the appearance of other gamma rays above and below 3.0 Mev in curve (b) is probably due to transitions feeding and leaving the 2.15- and 3.58-Mev levels of B^{10} .

Gamma-gamma coincidence spectra were also measured at a proton energy of 0.65 Mev. In this case the transition to the 5.16-Mev level of B^{10} has an energy of 2.00 Mev. Curves (a) and (b) in Fig. 16 show the spectra with the discriminating channel covering the energy interval from 1.92 to 2.12 Mev and from 2.28 to 2.48 Mev, respectively. Here again spurious effects occur, because the discriminating detector accepted to varying degrees transitions from the 2.15- and 3.58-Mev states of B^{10} . Nevertheless, there is an indication that coincident gamma rays of 3.0-, 2.1-, and 1.4-Mev energy occur more strongly in curve (a) than (b).

An attempt was made to make a quantitative

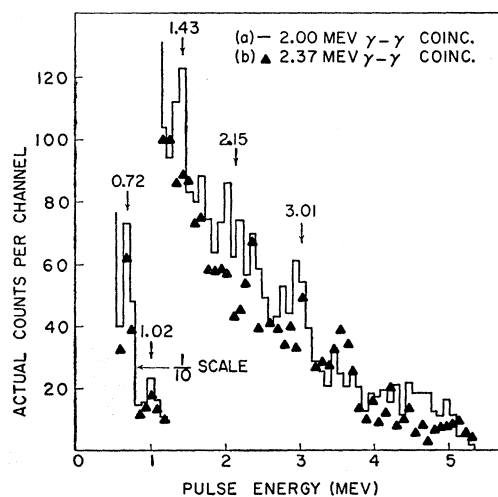


FIG. 16. Gamma-gamma coincidence spectra in $\text{Be}^9(p,\gamma)$ reaction at 0.65-Mev proton energy. The energies at which photopeaks are expected, if the capture gamma ray of 2.00 Mev leads to the 5.16-Mev state of B^{10} , are marked with arrows. See text for discussion.

analysis of Figs. 15 and 16, but it was found that the occurrence of the previously mentioned spurious effects made the analysis of no real value. All that can be said is that the 3.0-Mev coincident gamma ray has an intensity such that some finite fraction (within a factor of five of 1/10) of the 5.16-Mev level decays by gamma transition. The remaining decay of the 5.16 Mev occurs by alpha-particle emission.^{1,8} This result is consistent with previous estimates,¹ as well as with our findings in the singles gamma-ray spectra, which indicated the presence of 3.0-Mev gamma rays (from the 5.16-Mev state). The latter gamma rays had also been found by Bishop and Bizot⁷ in coincidence with 0.72-Mev gamma rays at a proton energy of about 0.6 Mev (thick target).

IV. INTERPRETATION OF RESULTS

(a) 0.33- and 0.99-Mev Resonances

In the proton energy range used in this experiment, the following resonances are known^{1,2} to occur (all widths given in c.m. system): 0.33 Mev, $\Gamma=130$ kev, $\Gamma_p=40$ kev, $J^\pi=1^-$; 0.98 Mev, $\Gamma\approx 80$ kev, $\Gamma_p\approx 70$ kev, $J^\pi=2^+$ (postulated by Mozer⁹; see also Dearnaly¹⁰); 0.99 Mev, $\Gamma=79$ kev, $\Gamma_p=50$ kev, $J^\pi=2^-$; 1.086 Mev, $\Gamma=\Gamma_p=2.7$ kev, $J^\pi=0^+$; 1.33 Mev, $\Gamma\approx 200$ kev, $\Gamma_p\approx 130$ kev, $J^\pi=2^-$. The 1.086-Mev resonance will be treated in Sec. (b) and no further reference will be made to it here.

In Figs. 5 to 11 we have indicated in dotted lines the shapes for the 0.33- and 0.99-Mev resonances calculated from the single-level Breit-Wigner formula using the above level parameters and others listed in reference 1, taking into account the variation of partial level widths with proton energy. It appears that in certain cases a nonresonant background is present; this process will be discussed in Sec. (c). For purpose of definitiveness, we have assumed that this background follows the shape $k^{-1}P_l$, where k is the proton (c.m.) propagation constant and P_l is the barrier penetration factor for angular momentum l . (The same radius parameter as in reference 1 was used.) In Table I we have collected the results for our resonant gamma-ray yields and compared these with the results of others^{3,5,7,11} (a comparison with reference 4 is made directly on Figs. 5 to

8). With the help of Figs. 5 to 11 and Table I we shall now discuss the individual excitation curves for the transitions to the B¹⁰ states.

Transition to the Ground State ($J^\pi=3^+$, $T=0$)—

See Fig. 5

The above parameters^{1,2} for the 0.99-Mev ($J^\pi=2^-$) resonance account very well for the cross section in the neighborhood of the resonance. Neglecting interference, we have subtracted the calculated curve from the experimental points and obtained the points shown as triangles. The latter points fit quite well on a Breit-Wigner curve calculated using the parameters of the 1.33-Mev resonance. However, this resonance has the same spin and parity² as the 0.99-Mev resonance and so must interfere, being destructive on one side of the resonance and constructive on the other. Introducing such interference terms destroys any resemblance between the calculated and experimental excitation function.

As no other broad resonance is definitely known in the energy region of interest (see, though, discussions in references 1 and 9 about possible s - and p -wave resonances between 0.35 and 0.98 Mev), we assign the excess yield at low energies to an s -wave nonresonant process, as discussed in Sec. (c). There remains then only the point at 1.2 Mev, which is several times too high to be explained by this nonresonant process. An explanation of this effect must await further studies of the proton capture in Be⁹ above 1 Mev.

The small angular anisotropies observed at about 0.4 Mev,⁷ 0.99 Mev,² as well as the data indicated in Fig. 5, are consistent with the above picture if small interference terms arising from d -wave protons are considered. The complete absence of the 0.33-Mev ($J^\pi=1^-$) resonance is clearly due to the natural weakness of the $M2$ radiation.

Mozer⁹ suggested that about 7 ev of the ground-state gamma-ray width at 0.99 Mev should be ascribed to the (2^+) 0.98-Mev resonance. This would reduce the $|M|^2$ value for the 0.99-Mev resonance in Table I by about 30%.

Transition to the 0.72-Mev State ($J^\pi=1^+$, $T=0$)—

See Fig. 6

This gamma ray is resonant at 0.33 Mev contrary³ to the isotopic spin selection rule for $E1$ transitions.¹² In addition, there is some nonresonant yield, which follows roughly an s - or p -wave penetrability curve, but our results are not precise enough to distinguish between these. The apparent absence of a resonance effect at 0.99 Mev is still consistent with the $|M|^2$ value for an $E1$ transition¹³; indeed the 0.33- and 0.99-

⁹ F. S. Mozer, Phys. Rev. **104**, 1386 (1956).

¹⁰ G. Dearnaly, Phil. Mag. **1**, 821 (1956). Mozer (reference 9) introduced a resonance at 0.98 Mev ($J^\pi=2^+$, $\Gamma\approx 80$ kev, $\Gamma_p/\Gamma\approx 0.9$, formed by channel spin 1) to explain the shape of the 1.086-Mev resonance observed in Be⁹(p,p) as well as the angular distributions in the neighborhood of 1 Mev. At the same time the anomalous correlation of the internal conversion pairs from Be⁹(p,γ) at 1 Mev [S. Devons and G. Goldring, Proc. Phys. Soc. (London) **A67**, 413 (1954)] was explained, while the near isotropy of the gamma radiation was retained by the channel spin restriction. On the other hand, Dearnaly made an independent investigation and analysis of Be⁹(p,p) and postulated a p -wave resonance near 1.1 Mev ($\Gamma\approx 200$ kev, Γ_p/Γ small) to explain the general form of the scattering curve above 1 Mev. We have assumed that the two p -wave resonances are the same, the detailed differences arising from the difficulty of analyzing proton scattering with a complicated set of resonances.

¹¹ R. R. Carlson and E. B. Nelson, Phys. Rev. **98**, 1310 (1955).

¹² L. A. Radicati, Phys. Rev. **87**, 521 (1952).

¹³ D. H. Wilkinson, Phil. Mag. **1**, 127 (1956); *Proceedings of the Rohovoh Conference on Nuclear Structure*, edited by H. J. Lipkin (North-Holland Publishing Company, Amsterdam, 1958), p. 175.

TABLE I. Resonant gamma-ray yields in $\text{Be}^9(p, \gamma)$ reaction at $E_p=0.33$ and 0.99 Mev (E_p =proton energy).

B ¹⁰ state (Mev) to which γ ray goes	$(d\sigma/d\Omega)(90^\circ)^a$ ($\mu\text{b}/4\pi$ sterad)	$E_p=0.33$ Mev (1 ⁻)			Γ_{γ^f} (ev)	$ M ^2 g$
		c	d	e		
0 (3 ⁺)	≤ 0.7	2.4	2.3		≤ 0.08	$\leq 8(M2)$
0.72 (1 ⁺)	6.4 ± 2	6	6	6	0.7 ± 0.2	$0.6\times 10^{-2}(E1)$
1.74 (0 ⁺)	15 ± 4	15 ^h	15 ^h	15 ^h	1.7 ± 0.5	$2.5\times 10^{-2}(E1)$
2.15 (1 ⁺)	4.5 ± 1.5	3	6.7	3	0.5 ± 0.2	$0.9\times 10^{-2}(E1)$
3.58 ⁱ (2 ⁺)	~ 1	5			~ 0.1	$\sim 0.5\times 10^{-2}(E1)$
5.16 (2 ^{-?})	$\leq 2.9^j$	3.6		3.7	≤ 0.32	$\leq 3(M1?)$
Secondary						
γ -ray (Mev)						
0.72	39 ± 8					
1.02	20 ± 5					
1.43	~ 10					
2.15	≤ 1					
2.8	≤ 1					

B ¹⁰ state (Mev) to which γ ray goes	$(d\sigma/d\Omega)(90^\circ)^a$ ($\mu\text{b}/4\pi$ sterad)	$E_p=0.99$ Mev (2 ⁻) ^k			Γ_{γ^f} (ev)	$ M ^2 g$
		Relative resonant yield (90°) ^l				
0 (3 ⁺)	400 ^h	400			23 ^h	$11\times 10^{-2}(E1)^m$
0.72 (1 ⁺)	≤ 10	≤ 30			≤ 0.6	$\leq 0.4\times 10^{-2}(E1)^m$
1.74 (0 ⁺)	19 ± 14	≤ 7			0.7 ± 0.5^n	$40\pm 30(E2)^n$
2.15 (1 ⁺)	22 ± 13	≤ 12			1.3 ± 0.8	$\sim 2\times 10^{-2}(E1)^m$
3.58 ⁱ (2 ⁺)	≤ 7				≤ 0.4	$\leq 1\times 10^{-2}(E1)^m$
5.16 (2 ^{-?})	$\leq 13^j$				≤ 0.8	$\leq 3(M1?)^m$
Secondary						
γ -ray (Mev)						
0.41		5.5 ± 0.6				
0.72	27 ± 15	49 ± 5				
1.02	22 ± 8	13 ± 2				
1.43	10 ± 8	~ 6				
2.15	≤ 2.5					
2.8	≤ 3					

^a Differential cross section at 90° to proton beam from present work, normalized to $400 \mu\text{b}/4\pi$ sterad, i.e., $\Gamma_\gamma=23$ ev (see reference 5), for the ground-state gamma ray at $E_p=0.99$ Mev (see reference 6).

^b These yields include the nonresonant as well as the resonant contributions. For a comparison of our results with those of reference 4, see Figs. 5 to 8.

^c See reference 7.

^d See reference 11.

^e See reference 3.

^f Calculated from present work assuming the partial and total level widths given in reference 1.

^g Ratio of gamma-ray width to Weisskopf estimate. See reference 13 for definitions. The assumed multipolarity of the gamma ray is given in parentheses.

^h Normalized to this value.

ⁱ The intensity of the capture transition to the 4.77-Mev state of B^{10} is less than or equal to that to the 3.58-Mev state.

^j The major part of this transition appears to go to the 5.16-Mev state; a small transition probability to the 5.11-Mev state is not excluded by our results.

^k The existence of an additional 2^+ state near $E_p=0.98$ Mev is postulated in reference 9 and appears to be indicated by the transition to the 1.74-Mev state. See text.

^l See reference 5. We assumed that the relative errors in intensity are one-half of the absolute errors given for the yields in this reference.

^m This value of $|M|^2$ does not take into account possible transitions from the 2^+ state at 7.5 Mev.

ⁿ Γ_γ and $|M|^2$ calculated for a transition from the 2^+ state, assuming the widths for this state given in reference 9, but neglecting a possible angular anisotropy (which would not affect the value within the stated error).

Mev resonances may have similar $|M|_{E1}^2$ values for this transition as well as for the others listed in Table I.

Transition to the 1.74-Mev State ($J^\pi=0^+$, $T=1$)— See Fig. 7

Up to a bombarding energy of about 0.8 Mev, the cross section follows the Breit-Wigner shape using the parameters of the 0.33-Mev resonance. Above 0.8 Mev there is clear evidence for another resonance. This cannot be the 0.99-Mev, $J^\pi=2^-$, resonance (or for that matter, the 1.33-Mev, $J^\pi=2^-$, resonance) since $\Gamma_\gamma \approx 0.7$ ev, which is about 1000 times too large for $M2$ radiation. We propose to identify this resonance with the p -wave resonance postulated by Mozer⁹ near 0.98 Mev ($\Gamma \approx 80$ kev) and by Dearnaly¹⁰ near 1.1 Mev ($\Gamma \approx 200$ kev). The accuracy of our points is not sufficient to distinguish between these energy values. For sake of definiteness

we have indicated on Fig. 7 a Breit-Wigner curve using Mozer's parameters, and have also used these parameters for calculating the gamma-ray width given in Table I. Doubling the width of the resonance (and moving it to a slightly higher energy to be consistent with the experimental points) would double the gamma-ray width, assuming Γ_p/Γ to be fixed.

The principal difficulty with this interpretation is the somewhat large $|M|_{E2}^2$ value which is calculated on the basis of the above assumptions. From the recent compilation of Wilkinson¹³ it appears, though, that $E2$ transitions in light nuclei may have $|M|^2$ values appreciably larger than unity.

We note that the 1.0-Mev resonance is also reflected in the excitation curves of the 0.72- and 1.02-Mev gamma rays (Fig. 11), which result mainly from the decay of the 1.74-Mev state. Since there is some direct

TABLE II. Resonant gamma-ray yields in Be⁹(*p*, γ) reaction at $E_p=1.086$ Mev.

Be ¹⁰ state (Mev) to which γ ray goes	Y (90°) ^a (relative)	Y^b ($\gamma/10^3 p$)	Γ_γ^c (ev)	$\Gamma_W(M1)^d$ (ev)
0 (3 ⁺)	≤ 0.03		≤ 0.2	9.1
0.72 (1 ⁺)	1.00 ^e	0.98 \pm 0.2	6.0 ^e	6.7
1.74 (0 ⁺)	$\leq 0.08(0.04\pm 0.02)^f$		$(0.2\pm 0.1)^f$	4.2
2.15 (1 ⁺)	$\leq 0.08(0.04\pm 0.02)^f$	≤ 0.05	$(0.2\pm 0.1)^f$	3.3
3.58 ^g (2 ⁺)	≤ 0.04		≤ 0.2	1.3
5.16 (2 ^{-?})	0.23 \pm 0.02 ^h	0.15 \pm 0.05	1.3 \pm 0.1	0.29
Secondary γ -ray (Mev)				
0.41		≤ 0.008		
0.72	1.5 \pm 0.4	1.08 \pm 0.2		
1.02	0.07 \pm 0.02	≤ 0.04		
1.43	0.03 \pm 0.01	~ 0.05		
2.15	≤ 0.07			
3.01	~ 0.03			

^a Relative differential cross section at 90° with respect to proton beam from present work.^b Absolute total yield from reference 5, calculated from yield at 90°, assuming isotropic cross section.^c Calculated assuming spin 0 for this resonance. For spin 1 the widths would be $\frac{1}{3}$ of the values given.^d $M1$ widths calculated from Weisskopf estimate. See reference 13 for definitions. For Be¹⁰ the estimates for $E1$ widths are 25 times the $M1$ widths.^e Normalized to this value.^f The values without parentheses are calculated from the capture gamma-ray intensities, the values in parentheses from the intensity balance of secondary gamma rays.^g The intensity of the capture transition to the 4.77-Mev state is less than or equal to that to the 3.58-Mev state.^h A small transition probability to the 5.11-Mev state is not excluded by our results.

feeding of the 0.72-Mev state, as well as some feeding of the 1.74-Mev state from the 2.15-Mev state,² the individual curves in Fig. 11 do not agree exactly with Fig. 7.

It may be of interest to note that according to Mozer⁹ the (2⁺) 0.98-Mev resonance is formed by channel spin 1, so that interference with 2⁻ resonances, formed by *s* waves, cannot occur. The high yield at 1.2 Mev (also indicated by Fig. 11, 1.02-Mev gamma ray) would again require the influence of higher lying resonances other than the (2⁻) 1.33-Mev resonance.

*Transition to the 2.15-Mev State ($J^\pi=1^+$, $T=0$)—
See Fig. 8*

This excitation curve is reflected in the excitation curve of the 1.43-Mev gamma ray (Fig. 11), since the 3.58-Mev state, which can also give a 1.43-Mev gamma ray,² is only weakly populated. It appears that the resonances at 0.33 and 0.99 Mev explain the entire curve adequately, although a small contribution from the 1.0-Mev *p*-wave resonance cannot be excluded. The $|M|_{E1}^2$ values for both resonances are normal and of similar magnitude.

The discrepancy with the curve of Edge and Gemmell⁴ might well be blamed on a difference in assumed gamma-ray detection efficiency and not on an angular anisotropy.

*Transition to the 3.58-Mev State ($J^\pi=2^+$, $T=0$)—
See Fig. 9*

A possible resonance at 0.33 Mev is indicated. The large angular anisotropy at 0.65 Mev suggests appreciable non-*s*-wave effects which are probably non-resonant. The apparent absence of a resonance at 0.99 Mev is still consistent with the $|M|_{E1}^2$ value at 0.33 Mev.

We find the intensity of this capture transition somewhat smaller than Bishop and Bizot,⁷ but it should be noted that the latter results were obtained from coincidence work in which—just as here—no correction for possible anisotropies was made. Also, a thick target was used.

It may be of interest to note that we have found no consistent evidence for capture transitions to the 4.77-Mev state. All we can say is that such capture transitions are not more intense than those to the 3.58-Mev state.

*Transition to the 5.16-Mev State ($J^\pi=2^+?$, $T=1?$)—
See Fig. 10*

We have noted previously in connection with Fig. 12 and the gamma-gamma coincidence work that the larger part of the radiation to the 5.1-Mev states appears to go to the 5.16-Mev state. It is clear from Fig. 10 that the known resonances play little part in the excitation curve for this capture gamma ray—at least at 90° with respect to the proton beam. The 0.33-Mev resonance may make a small contribution and the possibility of an interference effect with one of the resonances near 1.0 Mev exists, but the errors are too large for any real confidence about these matters. Perhaps the most important point is the large anisotropy at 0.65 Mev, which must be explained by whatever nonresonant process is used to describe the excitation curve [see Sec. (c)].

It should also be noted that our work obviates the difficulty of the $|M|_{M1}^2$ value at 0.33 Mev, previously believed³ to be anomalously large.

(b) 1.086-Mev Resonance

As mentioned earlier, we investigated the decay of the 1.086-Mev resonance, believed^{2,9} to be 0⁺. Table II

presents our results and compares them with those of Hornyak and Coor.⁵ A major point of disagreement with the latter work is the estimate of the intensity of the 1.02-Mev gamma ray, which, in our case, suggests that a transition occurs between the 7.56-Mev state of B^{10} (1.086-Mev resonance) and the 1.74-Mev state, known² to have a spin 0^+ ($T=1$). Indication for the same transition was pointed out in connection with Fig. 13 (note that the "off-resonant background" does not influence the shape of the spectrum in the critical region around 5.8 Mev).

Further indication of inconsistency in connection with this resonance is given by the low yield given in reference 5 for the 0.41-Mev secondary gamma ray, which should have an intensity comparable to the 1.43-Mev gamma ray (see reference 2), even allowing for the maximum possible feeding of the 3.58-Mev level, given in Table II. (Only strong angular anisotropy effects could account for this discrepancy, which would not allow a 0^+ spin assignment for the 7.56-Mev state.)

A third indication of inconsistency with a 0^+ spin assignment for this resonance comes from the strength of the transition to the 5.16-Mev state (see Table II). The radiation width is far too large for $E2$ radiation ($|M|^2 \approx 10^4$) and large even for $M1$ radiation, although it should be noted that a possible angular anisotropy of this gamma radiation has not been taken into account. (The previously determined² small upper limit for the anisotropy refers mainly to the capture gamma ray to the 0.72-Mev state.) It is clear, though, that $\Delta J = \pm 1$ for this transition and hence the $J=0$ assignment to the 7.56-Mev level or the $J=2$ assignment for the 5.16 Mev (or both) must be in error.

Without doing further work on this resonance it is not possible to give an explanation of the experimental facts which is consistent with reasonable decay characteristics and the isotopic spin selection rules.^{12,14} For example, one could assume $J^\pi = 0^+$, $T=1$ for the 7.56-Mev level and $J^\pi = 1^\pm$, $T=0$ for the 5.16-Mev level. This would be consistent with the elastic proton scattering, the 6.84-Mev gamma-ray width of and isotropy from the 7.56-Mev level, as well as the absence of deuteron and alpha decay,² but leave unexplained the small alpha width of the 5.16-Mev level.¹ On the other hand one could assume $T=1$ (and hence¹ $J^\pi = 2^+$) for the 5.16-Mev level to explain the small alpha width and assign $J^\pi = 1^\pm$, $T=0$ to the 7.56-Mev level. This could possibly be consistent with the elastic proton scattering,¹⁵ but in turn does not explain the small alpha and deuteron widths of the 7.56-Mev level. $J^\pi = 2^-$, $T=0$ and $J^\pi = 1^+$, $T=1$ assignments for the 5.16- and 7.56-Mev levels, respectively (with an isotopic-spin purity of better than $1:10^4$ for the latter level) could give a consistent account¹⁶ of the experi-

mental facts, except for leaving unexplained the small alpha width of the 5.16-Mev state.

(c) Nonresonant Capture

The excitation functions for capture radiation to the states at 0, 0.72, 3.58, and 5.16 Mev (Figs. 5, 6, 9, and 10) show characteristics that may perhaps be better described in terms of a nonresonant process rather than by introducing remote broad resonances. It should be borne in mind, though, that in the $Be^9(p,d)$, as well as the $Be^9(p,\alpha)$, reaction¹⁷ there appear interference effects characteristic of levels of opposite parity between the 0.33- and 0.99-Mev resonances, which have not as yet been explained in detail.² Furthermore the peak of the "1-Mev resonance" in these reactions is at 0.93 Mev,¹⁸ which may also be due to interference effects between several levels.

The nonresonant process we have in mind is the direct capture process¹⁹ which has been observed most clearly in $O^{16}(p,\gamma)$. This reaction has been interpreted in detail²⁰ as a direct electric dipole transition from the initial state of an incident proton wave to the final state of a bound orbit. No compound nucleus is formed and in fact the nuclear region itself plays very little part in the reaction. The consequences of this simple model are as follows:

(1) The cross section for energies below the Coulomb barrier is roughly proportional to the penetrability, although not to an accuracy that would allow a distinction between s -wave and p -wave capture without detailed calculation.

(2) Multipoles other than $E1$ can be neglected since the $E1$ strength is not inhibited by isotopic spin or other considerations and the parity can always be arranged by selecting the appropriate partial wave of the incident proton.

(3) The angular distribution is always isotropic for s -wave proton capture. For incident p -waves radiating to an s -wave orbit the angular distribution is $\sin^2\theta$.¹⁹ If the final state is to be described as a d -wave orbit, the anisotropy would be $\sim 30\%$ which would hardly be distinguished from isotropy in our measurements.

(4) The most favored final states for direct radiative capture are those with large proton reduced widths and small binding energies.

The low-lying even-parity states of B^{10} can be ex-

mixture of the capture radiation (amplitude ratio $\approx -\frac{1}{6}$), or by the preference for channel spin 2 in the proton capture. The Weisskopf estimate for the expected $E2$ transition width to the ground state is only 0.06 ev. Alpha-particle and deuteron emission from this state would be suppressed by the isotopic spin selection rule. Note that $T=1$ is likely for this state in any case in view of Mörpurgo's selection rule (reference 14) [D. H. Wilkinson (private communication)]; E. K. Warburton, Phys. Rev. **113**, 595 (1959).

¹⁷ Neuendorffer, Inglis, and Hanna, Phys. Rev. **82**, 75 (1951).

¹⁸ Weber, Davis, and Marion, Phys. Rev. **104**, 1307 (1956).

¹⁹ Warren, Laurie, James, and Erdman, Can. J. Phys. **32**, 563 (1954); N. W. Tanner, Phys. Rev. **114**, 1060 (1959).

²⁰ R. F. Christy and I. M. Duck (to be published).

¹⁴ G. Mörpurgo, Phys. Rev. **110**, 721 (1958).

¹⁵ F. S. Mozer (private communication).

¹⁶ The apparent angular isotropy² of the radiation to and from the 0.72-Mev state could be explained by appropriate $E2/M1$

pressed for our purpose as Be⁹ plus a *p*-state proton. Similarly the odd-parity states would be Be⁹ plus an *s*-state or *d*-state proton (probably a mixture). Hence we expect direct capture to the *even* states to result from *s*-wave incident protons, and direct capture to the *odd* states from *p*-wave incident protons, i.e., the parity of the *E1* operator cancels the parity of the Be⁹ target nucleus.

The nonresonant ground-state transition is in fact almost isotropic (Fig. 5) in accord with this model and the even parity of the ground state. On the other hand the transitions to the 3.58- and 5.16-Mev states are considerably anisotropic (at least at one proton energy—see Figs. 9 and 10) implying odd parity for these states contrary to other evidence.² Possibly the anisotropy to the 3.58-Mev state should not be taken too seriously as the errors are very large. For the 5.16-Mev state $d\sigma/d\Omega(90^\circ):d\sigma/d\Omega(0^\circ)\approx 5$.|| This is very difficult to reconcile with any angular distribution less violent than $\sin^2\theta$, especially when correction is made for counter solid angle. In particular the unresolved contribution of a transition to the 5.11-Mev, $J^\pi=2^-$ (?),¹ state, which might be inferred from Fig. 12, could hardly be large enough to account for the strong asymmetry.

If the 5.16-Mev state does have odd parity, then it seems the only reasonable⁸ assignment is $J^\pi=2^-$, $T=0$. From Sec. (b) it follows that the 1.086-Mev resonance must have $J^\pi=1^+$, $T=1$. As stated there, the great difficulty remaining is to explain the small alpha width of the 5.16-Mev state. It is noted that these assignments do not lead us into any very serious violation of either the *E1* or *M1* isotopic spin selection rules.^{12,14,16} Also, the failure⁸ of the 5.16-Mev state to radiate to the 1.74-Mev state is explained. It is clear, though, that more measurements, particularly of gamma-ray angular distributions, are needed to verify these speculations.

V. CONCLUSIONS

Our original hope in this experiment, i.e., to find evidence for another 1⁻ level which could explain the

high isotopic-spin impurity³ of the (1⁻) 6.89-Mev state, was not fulfilled. In particular, the 7.01-Mev anomaly² suggested in reference 1 as a possible candidate for this level did not appear in the (*p*, γ) excitation functions, presumably because its proton width is very small. On the other hand evidence was found, which points to the existence of a 7.5-Mev state, formed by *p* waves, as postulated by Mozer⁹ and Dearnaly.¹⁰

Our work has indicated some evidence which is inconsistent with the previous spin-parity assignments for the 5.16- and 7.56-Mev states, although we believe that further work is needed to clarify the exact state of affairs. Tentatively we assign $J^\pi=2^-$, $T=0$ to the 5.16-Mev level, leaving its small alpha width unexplained. The evidence previously adduced¹ for assigning a negative parity to 5.11-Mev state is not necessarily invalidated by these assignments. Kurath's work²¹ then demands that $J^\pi=2^+$, $T=1$ for the 4.77-Mev state.

Finally, large nonresonant contributions to the capture process in the Be⁹(*p*, γ) reaction have been found for transitions to the higher excited states, in addition to the ground state.⁴ The mechanism of the nonresonant capture is believed by us to be direct radiative capture^{19,20} and has led us tentatively to assign odd parity to the 5.16-Mev state of B¹⁰.

ACKNOWLEDGMENTS

Two of us (W. E. M. and C. M. H.) would like to express our gratitude to Professor C. C. Lauritsen for allowing us to work at the Kellogg Radiation Laboratory of the California Institute of Technology. The encouragement of Professor W. A. Fowler as well as discussions with Dr. A. B. Clegg, Dr. G. Dearnaly, Dr. S. S. Hanna, Dr. G. A. Jones, and Professor D. H. Wilkinson are gratefully acknowledged. We appreciate very much the loan of equipment and help received from Dr. R. W. Kavanagh. Also, one of us (W. E. M.) is very grateful to the Alfred P. Sloan Foundation for the grant of a fellowship during 1957–1958, which made this work possible, and for other support.

|| *Note added in proof.*—Recent measurements of the angular anisotropy of the gamma-rays leading to the 5.1-Mev states in B¹⁰ with respect to the proton beam (at 0.65 Mev) indicate a value considerably less than found here, which would invalidate the argument for the negative parity of the 5.16-Mev state (N. W. Tanner and S. S. Hanna, private communication).

²¹ D. Kurath, Phys. Rev. **101**, 216 (1956); *Proceedings of the Rehovoth Conference on Nuclear Structure*, edited by H. J. Lipkin (North-Holland Publishing Company, Amsterdam, 1958), p. 46. It is of interest to note that according to the latter reference, the 4.77-Mev state has the decay characteristics computed for the $T=1$ state, but not the 5.16-Mev state.